CVaR constrained planning of renewable generation with consideration of system inertial response, reserve services and demand participation

Andrés Inzunza [a], Rodrigo Moreno [b,c,*], Alejandro Bernales [d], Hugh Rudnick [a]

[a] Dept. of Electrical Engineering, Pontificia Universidad Católica de Chile, Macul, Santiago 7820436, Chile
[b] Dept. of Electrical Engineering (Energy Centre), Universidad de Chile, Santiago 8370451, Chile
[c] Dept. of Electrical and Electronic Engineering, Imperial College London, London SW7 2AZ, UK
[d] Dept. of Industrial Engineering, Universidad de Chile, Santiago 8370439, Chile

ABSTRACT

Integration of renewable generation can lead to both diversification of energy sources (which can improve the overall economic performance of the power sector) and cost increase due to the need for further resources to provide flexibility and thus secure operation from unpredictable, variable and asynchronous generation. In this context, we propose a cost-risk model that can properly plan generation and determine efficient technology portfolios through balancing the benefits of energy source diversification and cost of security of supply through the provision of various generation frequency control and demand side services, including preservation of system inertia levels. We do so through a scenario-based cost minimization framework where the conditional value at risk (CVaR), associated with costs under extreme scenarios of fossil fuel prices combined with hydrological inflows, is constrained. The model can tackle problems with large data sets (e.g. 8760 hours and 1000 scenarios) since we use linear programming and propose a Benders-based method adapted to deal with CVaR constraints in the master problem. Through several analyses, including the Chilean main electricity system, we demonstrate the effects of renewables on hedging both fossil fuel and hydrological risks; effects of security of supply on costs, risks and renewable investment; and the importance of demand side services in limiting risk exposure of generation portfolios through encouraging risk mitigating renewable generation investment.

© 2016 Elsevier B.V. All rights reserved.

1. Introduction

1.1. Motivation

Integration of renewable generation may support not only development of sustainable electricity systems but also diversification of energy sources, improving the overall economic performance of the power sector (Awerbuch, 2006; Jansen et al., 2006; Doherty et al., 2006; Delarue et al., 2011). In fact, an electricity system which is less dependent on thermal and hydroelectric plants may decrease its exposure to volatile fossil fuel prices and hydrological conditions driven by market and climate phenomena, reducing risks levels associated with generation investment and operating costs. Hence, policy makers and planners that are more risk averse may perceive higher economic benefits from renewable generation technologies (Awerbuch, 2006).

Integration of renewable generation, however, may significantly escalate capital and operating costs due to the need for further resources to provide flexibility and thus secure operation from unpredictable,

variable/intermittent and asynchronous generation. Therefore, a cost-benefit analysis to determine renewable generation investment from a system perspective should be able to balance the various benefits and costs associated with diversification of energy sources, security of supply, system-wide investment and operational costs, etc.

1.2. Literature review and contribution

From a socio-economic viewpoint, the integration of renewable technologies for electricity generation presents various advantages and disadvantages that need to be properly balanced. For example, electricity generation from renewables can make local electricity markets less dependent on international fossil-fuel markets (Awerbuch, 2006; Jansen et al., 2006; Doherty et al., 2006; Delarue et al., 2011), and can also yield significant environmental benefits in terms of reductions in CO_2 and other greenhouse gas emissions (that are the main responsible for global warming) (Pindyck, 2013), displacing the need for fossil-fuels energy production. On the other hand, renewable technologies can also cause problems in terms of security of supply due to, as discussed in Denholm and Margolis (2007), Joskow (2011), their intermittent production of power (e.g. a plant based on solar technology produces

---

* Corresponding author at: Tupper 2007, Santiago 8370451, Chile.
E-mail address: rmorenovieyra@ing.uchile.cl (R. Moreno).

Nomenclature

Sets

I:	Set of all generation technologies
I^{RH}:	Set of all types of hydro reservoir technologies (subset of I^{NR})
I^{FS}:	Set of fast start technologies participating in standing reserves (subset of I)
I^{NR}:	Set of non-renewable technologies (subset of I)
I^{G}:	Set of technologies that participate in primary frequency control (subset of I^{NR})
I^{NG}:	Set of technologies that do not participate in primary frequency control (subset of I^{NR})
I^{R}:	Set of renewable technologies (subset of I)
J:	Set of hours in a year
J_k^D:	Set of hours in a particular day k (subset of J)
K:	Set of days in a year
S:	Set of simulation scenarios

Parameters

CV:	Required (maximum) CVaR of generation portfolio costs, [\$]
D_j:	Demand in hour j, [MWh]
dc^-:	Cost of demand decrease due to demand shifting, [\$/MW]
dc^+:	Cost of demand increase due to demand shifting, [\$/MW]
$DR_{j,s}^S$:	Amount of curtailable demand in hour j under scenario s for the operating reserve timeframe, [MW]
$DR_{j,s}^P$:	Amount of curtailable demand in hour j under scenario s for the primary frequency control timeframe, [MW]
$\overline{ds^-}$:	Maximum fraction of demand in any hour that can be shifted/decreased, [p.u.]
$\overline{ds^+}$:	Maximum fraction of demand in any hour that can be shifted/increased, [p.u.]
f^0:	Nominal system frequency, [Hz]
f^{db}:	Governors' frequency dead band, [Hz]
f^{min}:	Minimum frequency allowed under an N-1 contingency, [Hz]
FS:	Fraction of fast start generation capacity that contributes to operating reserves, [p.u.]
$FU_{i,s}$:	Fuel cost of technology i in scenario s, [\$/MWh]
H_f:	Inertia constant of failed unit, [s]
H_i:	Inertia constant of units of technology i, [s]
$Inf_{i,j,s}$	Normalized water inflow of reservoir i in hour j under scenario s, [hm^3/MW]
$INV_{i,s}$:	Annuitized investment cost of technology i under scenario s (this includes yearly fixed maintenance costs), [\$/MW-year]
$\overline{P}_i, \underline{P}_i$:	Maximum and minimum power output of each unit of technology i, [MW]
p_s:	Probability of occurrence of scenario s, [p.u.]
r_i:	Emergency ramp rate of a unit of technology i, [MW/s]
$RP_{i,j}$	Generation availability of renewable technology i at hour j, [p.u.]
$RRP_{j,s}$:	Run-of-river generation availability at hour j in scenario s, [p.u.]
t^{SR}:	Maximum time in which spinning reserves must be deployed, [h]
$\underline{v}_i, \overline{v}_i$:	Normalized lower and upper bound of stored water in reservoir i, [hm^3/MW]
α:	CVaR parameter that defines the $(1-\alpha)\%$ highest cost scenarios, [p.u.]
$voll$:	Value of lost load, [\$/MWh]
λ_i:	Losses of stored water due to evaporation and/or seepage in reservoir i, [p.u.]

ΔP:	Maximum N-1 contingency magnitude for which reserve and inertia requirements are set, [MW]
η_i:	Production coefficient of reservoir i, [MWh/hm^3]
ρ_i:	Hourly ramp rate limit of technology i, [MW/h]
$\sigma_{SOL,j}$:	Standard deviation of solar forecast errors in hour j, [p.u.]
σ_{WND}:	Standard deviation of wind forecast errors in all hours, [p.u.]

Decision variables

c_i:	Installed capacity of technology i, [MW]
C_s:	Total investment and operating costs in scenario s (without including the value of lost load), [\$]
$\widetilde{C}_s$:	Total investment and operating costs in scenario s (including the value of lost load), [\$]
$D_{j,s}^-$:	Demand decrease in hour j under scenario s due to demand shifting, [MW]
$D_{j,s}^+$:	Demand increase in hour j under scenario s due to demand shifting, [MW]
d_s:	α – CVaR (auxiliary) variable that represents the positive deviation of the cost in scenario s with respect to the value of variable z, [\$]
$g_{i,j,s}$:	Generation of technology i in hour j under scenario s, [MWh]
$LL_{j,s}$:	Lost load in hour j under scenario s, [MWh]
$n_{i,j,s}$:	Number of online or synchronized units of technology i in hour j under scenario s, [−]
$R_{i,j,s}^P$:	Capacity headroom in units of technology i in hour j under scenario s for primary frequency response, [MW]
$R_{i,j,s}^S$:	Capacity headroom in units of technology i in hour j under scenario s for spinning reserve, [MW]
$v_{i,j,s}$:	Volume of stored water in reservoir i at the end of hour j under scenario s, [hm^3]
$sp_{i,j,s}$:	Water lost through spillage in hour j under scenario s by hydro reservoir technology i, [hm^3]
z:	α – CVaR (auxiliary) variable that represents $VaR_\alpha(\widetilde{C}_s)$, [\$]

electricity only when the sun is shining). To minimize the effect of large amount of renewable generation on reliability, operators of electricity systems use additional generation reserves (i.e. backup generation based on other – usually conventional – technologies) to maintain system security at acceptable levels (Gowrisankaran et al., 2011; Borenstein, 2012).

Despite the evident aforementioned challenges associated with electricity systems, cost-benefit optimization models that determine generation expansion have historically been undertaken without considering a risk position from the planner and security measures to ensure a reliable supply (such as reserves, see for instance Steffen and Weber (2013), Neuhoff et al. (2008), Eide et al. (2014)); and although this has been accepted to plan conventional systems (due to their simpler characteristics such as the presence of fully controllable generation resources, slow dynamics associated with demand changes, reliable power generation, etc.), there is an increasing interest from policy makers to (i) reduce dependency levels on international markets through generation technology diversification and investment in renewables, and (ii) maintain system reliability (at acceptable levels) when large amounts of renewables are connected.

To capture the effects of generation resource diversification, we need to develop generation expansion models based on portfolio theory, whose principles were introduced by Markowitz (1952). In this framework, the optimal generation expansion problem can be understood as a portfolio optimization, where asset allocations represent the optimal investment in different generation technologies (including renewable

and fossil fuel technologies). The first application of portfolio theory to optimal generation planning was developed in 1972 by Bar-Lev and Katz (1976) that considered fossil-fuel plants only and neglected security of supply constraints. More recent studies have developed cost-risk approaches that use Gaussian distributions to capture uncertainty and standard deviations to measure risks. The first studies of this kind were based on capacity-only models (Awerbuch and Berger, 2003), and demonstrated that displacement of conventional generation capacity through integration of renewables can effectively contribute to reduce risks associated with generation investment and operating costs (associated with volatile fossil-fuel prices), albeit the overall average cost can be increased. Later on, studies like those in Huang and Wu (2008), Gotham et al. (2009), Vithayasrichareon and MacGill (2014) introduced operational aspects associated with intermittent renewables, recognizing that such intermittency reduces the value of renewable generation capacity. Recently, reference Delarue et al. (2011) has considered more detailed operational constraints related to system's ability to ramp flexibly and thus efficiently absorb changes from intermittent renewables' output. This study demonstrates that the increased need for flexibility that allows system operators to deal with intermittent generation can affect investment in technologies such as wind and solar, reducing further their share with respect to portfolios obtained from studies in which system flexibility was not captured.

In this context, recent studies suggest that an array of flexible measures to secure system operation through, for example, higher volumes of generation reserves and demand side services, have to be in place in order to promote increased levels of investment in renewables (Strbac, 2008; De Jonghe et al., 2010; Pérez-Arriaga and Battle, 2012). Clearly, these sources of flexibility will need to be properly planned, including detailed constraints in relation to reserve services (such as the need for primary frequency response (PFR) as proposed in Chávez et al. (2014), spinning and standing reserves). Hence, we contribute with a novel cost-risk model to determine efficient generation technology portfolios, which can:

- Properly balance the benefits of energy source diversification and cost of security of supply (representing in detail the provision of various ancillary services, such as generation frequency control and demand side services, including preservation of system inertia levels);
- Determine risks from more realistic scenarios rather than from standard deviations of simplified Gaussian distributions; and
- Tackle a large input data set (e.g. 1000 scenarios over 8760 hours) as we propose an efficient Benders-based method (that can be run using parallel processing) for minimizing cost expectation subject to CVaR constraint in a linear programming (LP) fashion.

Through several analyses, including the main Chilean electricity system, we demonstrate the importance of renewables in hedging both fossil fuel and hydrological risks and confirm that approaches that ignore risks will significantly undermine the value of renewables to diversify energy sources. We also show the effect of security of supply on increasing costs and risks, and constraining renewables investment. In this context, we highlight the importance of demand side actions which can encourage higher volumes of investment in risk mitigating renewable generation capacity. The concepts developed in this paper can be broadly applied on both thermal and hydro-thermal electricity systems, albeit these are particularly relevant for countries such as Chile, Peru, Brazil, Russia, China, Canada, India, Indonesia and Nepal (World Energy Council, 2015), where existing capacity and potential of hydropower generation requires a combined treatment of risks from both prices of fossil fuels and hydrological conditions for the analysis of long-term generation investment scenarios.

This paper is structured as follows. Section 2 presents the cost-risk model to determine optimum portfolios of electricity generation. Sections 3 and 4 present and discuss the main results over a small and a large-scale system in order to illustrate/validate, and prove scalability of our model, respectively. Section 5 concludes.

2. The model

2.1. Overview

We propose a two-stage stochastic linear programming model to determine the optimum portfolio of generation technologies of a future power system. The model minimizes overall expectation of investment and operating costs across a large number of future scenarios subject to a given level of CVaR associated with these costs. To do so, we optimize the vector of generation capacities in a first stage, and the operation of the proposed generation infrastructure in a second stage, which are coordinated by a Benders-based method due to the large size of the problem (e.g. 8760 hours a year under hundreds of scenarios). At the operational stage, complexities related to maintaining system security levels through scheduling various types of reserves from generation and demand, are considered (including effects in system inertial response).

Therefore, the model can balance investment in conventional and renewable generation in order to minimize overall system costs subject to a given risk exposure due to unexpected fossil fuel prices and/or hydrological conditions. Hence investment in renewables may be preferred despite their higher investment costs, if fuel prices associated with thermal plants are highly volatile. Also, the model can recognize escalation in operating costs due to increased reserve requirements to deal with uncertainty associated with the output of renewable generation. Furthermore, under low demand conditions, renewables' output might be curtailed and fast thermal plants (rather than low-cost thermal units) can result scheduled despite its higher costs, if increased availability of renewable resources such as wind and solar deteriorates system inertial response and thus jeopardizes security of supply. Under these conditions, the model can conciliate secure operation and renewables' output maximization that minimizes cost.

Hence our model can suggest portfolios of generation investment that are more robust against fossil fuel prices and hydrological conditions that can significantly change from one year to another. In addition, such portfolios consider further resources needed to secure system operation against renewables' output uncertainty and their associated operating cost. Indeed, the model can handle both long-term uncertainty due to changing fuel prices and hydrological conditions, and short-term uncertainty due to renewables' output fluctuations.

2.2. Risk constrained optimization model

2.2.1. CVaR representation

The model determines the installed capacity of generation and its associated dispatch by minimizing expected investment and operation costs across a set of scenarios (that can represent combination of fossil fuels prices and hydrological inflows, for example) constrained to a level of risk exposure in terms of CVaR. Since demand is considered inelastic, maximum social welfare is reached when total cost is minimized as shown in Eqs. (1) and (2).

$$\text{O.F.} : \quad \min \sum_{s \in S} p_s \cdot C_s + \sum_{s \in S} p_s \cdot \text{voll} \cdot \sum_{j \in J} LL_{j,s} \tag{1}$$

s.t.:

$$C_s = \sum_{j \in J} D^-_{j,s} \cdot dc^- + \sum_{j \in J} D^+_{j,s} \cdot dc^+ + \sum_{i \in I} \text{INV}_{i,s} \cdot c_i + \sum_{i \in I} \sum_{j \in J} \text{FU}_{i,s} \cdot g_{i,j,s} \qquad \forall s \in S \tag{2}$$

α-CVaR constraints are used as proposed in reference Rockafellar and Uryasev (2002), which are shown in Eqs.(3)–(5). A large *CV* value (i.e. α-CVaR upper bound) can be used to obtain the minimum cost portfolio. Several lower values of *CV* can be used to draw the Pareto

boundary between minimum expectation and minimum risk solutions.

$$\widetilde{C}_s = C_s + \text{voll} \cdot \sum_{j \in J} LL_{j,s} \qquad \forall s \in S \tag{3}$$

$$d_s \geq \widetilde{C}_s - z \qquad \forall s \in S \tag{4}$$

$$z + \frac{1}{1-\alpha} \sum_{s \in S} d_s \cdot p_s \leq CV \tag{5}$$

2.2.2. Economic dispatch constraints

Eq. (6) ensures that generation and load are balanced in every period (e.g. one hour), including load that can be curtailed or lost under extreme scenarios, e.g. dry inflows, and demand shifted used to accommodate the output of renewables. Eqs. (7) and (8) limit the amount of flexible demand in every period to be lower than or equal to a percentage of the demand. Eq. (9) ensures that changes in load due to flexible demand shifts are balanced within a time window, e.g. 24 hours.

$$\sum_{i \in I} g_{i,j,s} = D_j + D_{j,s}^+ - D_{j,s}^- - LL_{j,s} \qquad \forall j \in J, s \in S \tag{6}$$

$$D_{j,s}^- \leq \overline{ds^-} \cdot D_j \qquad \forall j \in J, s \in S \tag{7}$$

$$D_{j,s}^+ \leq \overline{ds^+} \cdot D_j \qquad \forall j \in J, s \in S \tag{8}$$

$$\sum_{j \in J_k^D} D_{j,s}^+ - \sum_{j \in J_k^D} D_{j,s}^- = 0 \qquad \forall k \in K, s \in S \tag{9}$$

Eqs. (10) and (11) are used to model hydro power plants that may store energy in the form of water resources. Eq. (10) considers water inflows, and outflows associated with generation, spillage and losses that may depend on seepage and evaporation. Eq. (11) limits the volumes of stored water. An average rather than an overhead dependent η_i is used and this is a reasonable assumption for system planning studies as considered in Gil et al. (2014). Further constraints that bound initial and final reservoir levels and represent actual system operator's practices are, for simplicity, omitted in this paper.

$$v_{i,j,s} = v_{i,j-1,s} + \text{inf}_{i,j,s} \cdot c_i - \frac{g_{i,j,s}}{\eta_i} - sp_{i,j,s} - v_{i,j,s} \cdot \lambda_i \qquad \forall i \in I^{RH}, j \in J, s \in S \tag{10}$$

$$v_{i,j,s} \leq c_i \cdot \overline{v}_i \qquad \forall i \in I^{RH}, j \in J, s \in S \tag{11}$$

Regarding run-of-river plants, the model constrains their production and reserve provision according to normalized hourly profiles which depend on hydrological scenarios as shown in Eq. (12).

$$R_{RIV,j,s}^S + g_{RIV,j,s} \leq RRP_{j,s} \cdot c_{RIV} \qquad \forall j \in J, s \in S \tag{12}$$

It is important to mention at this point that our proposed model can be broadly applied on both thermal and hydro-thermal electricity systems since the model can be easily accommodated to study thermal systems by neglecting those constraints associated with hydro resources.

Units' ramp rates limits are shown in Eqs. (13) and (14) which constrain the amount of power production that can be increased or decreased from one period to the next one. To properly constrain ramp rates, we need to determine the number of units that are synchronized (i.e. online units) as shown in Eqs. (15)–(17). Also, we use function $min\{\}$ and $\underline{P}_i$ in order to recognize that a net increase/decrease in generation output may be accompanied by a potential reduction/growth in the

number of synchronized units.

$$g_{i,j,s} - g_{i,j-1,s} \leq \min\{n_{i,j,s}, n_{i,j-1,s}\} \cdot \rho_i + (n_{i,j,s} - n_{i,j-1,s}) \cdot \underline{P}_i \qquad \forall i \in I^{NR}, j > 1 \in J, s \in S \tag{13}$$

$$g_{i,j-1,s} - g_{i,j,s} \leq \min\{n_{i,j,s}, n_{i,j-1,s}\} \cdot \rho_i + (n_{i,j-1,s} - n_{i,j,s}) \cdot \underline{P}_i \qquad \forall i \in I^{NR}, j > 1 \in J, s \in S \tag{14}$$

$$n_{i,j,s} \cdot \underline{P}_i \leq g_{i,j,s} \leq n_{i,j,s} \cdot \overline{P}_i \qquad \forall i \in I^{NR}, j \in J, s \in S \tag{15}$$

$$n_{i,j,s} \cdot \overline{P}_i \leq c_i \qquad \forall i \in I^{NR}, j \in J, s \in S \tag{16}$$

$$n_{i,j,s} \in \mathbb{Z} \qquad \forall i \in I^{NR}, j \in J, s \in S \tag{17}$$

Eq. (18) limits renewables' output according to the volume of renewable resources available which are modeled through normalized hourly profiles that multiply installed capacity levels. Installed capacity of these technologies is aggregated into several types, for instance, wind and solar. It is not relevant to identify the number of synchronized units for these technologies.

$$g_{i,j,s} \leq RP_{i,j} \cdot c_i \qquad \forall i \in I^R, j \in J, s \in S \tag{18}$$

2.2.3. Security of supply through inertial frequency response and reserves

We extended the simplified dynamic model of primary frequency response (PFR) developed in reference Chávez et al. (2014) in order to deal with system planning. Following definitions in Chávez et al. (2014), PFR is considered adequate if system frequency does not drop below a given limit after any single generation contingency. Reserve maintained for PFR is referred to as primary reserve.

Eq. (9) in Chávez et al. (2014) shows that the minimum system ramp C_{MIN} that ensures frequency to be above a given level f_{MIN} (considering post-contingency inertia of the system $M_H = 2E_0/f_0$, magnitude of the largest contingency P_l, the nominal frequency f_0, the post-contingency system kinetic energy E_0, and governors frequency dead-bands f_{db} assumed to be equal for all governors), has to comply with Eq. (19):

$$C_{MIN} \cdot E_0 = \frac{\frac{1}{4} P_l^2}{\left(1 - \frac{f_{MIN}}{f_0} - \frac{f_{db}}{f_0}\right)} \tag{19}$$

Hence we can re-write Eq. (19) as Eq. (20) under the assumptions that: (i) units' governors respond with a constant (and conservative) ramp rate, and (ii) units responding to the frequency drop do not reach their maximum output while the power balance has not been restored. These are the same assumptions made in reference Chávez et al. (2014) and we ensure that maximum output is not reached by adding Eqs. (21) and (22).

$$\left(\sum_{i \in I^G} n_{i,j,s} \cdot r_i\right) \cdot \left(\sum_{i \in I^{NR}} H_i \cdot n_{i,j,s} \cdot \overline{P}_i - H_f \cdot \Delta P\right) \geq \frac{\frac{1}{4}\left(\Delta P - DR_{j,s}^P\right)^2}{\left(1 - \frac{f^{min}}{f^0} - \frac{f^{db}}{f^0}\right)} \qquad \forall j \in J, s \in S \tag{20}$$

$$\sum_{i \in I^G} R_{i,j,s}^P \geq \Delta P - DR_{j,s}^P \qquad \forall j \in J, s \in S \tag{21}$$

$$R_{i,j,s}^P \leq n_{i,j,s} \cdot r_i \cdot \left(\frac{\Delta P - DR_{j,s}^P}{\sum_{i \in I^G} n_{i,j,s} \cdot r_i}\right) \qquad \forall i \in I^G, j \in J, s \in S \tag{22}$$

In Eqs. (20) and (22) expression $\sum_{i \in I^G} n_{i,j,s} \cdot r_i$ corresponds to the system ramp after the fault occurs and $\sum_{i \in I^{NR}} H_i \cdot n_{i,j,s} \cdot P_i - H_f \cdot \Delta P$ is equal to the post contingency system kinetic energy. Expression $\Delta P - DR_{j,s}^P$ represents the power output of the largest fault, minus the contribution of demand to reduce this power which is considered to occur instantly.

Eq. (21) ensures there is enough generation reserve or headroom (i.e. generation capacity needed to be kept unused in order to enable production of post-fault power) to deal with the fault, and Eq. (22) sets an upper bound to the reserve maintained in each technology. The latter is necessary to ensure that primary reserve is deployable before frequency reaches its nadir at time $(\Delta P - DR^P_{j,s})/(\sum_{i \in I^G} n_{i,j,s} \cdot r_i)$. It is worthwhile to mention that in this context, we use emergency ramp rates (or generation frequency response rates) r_i rather than hourly ramp rates ρ_i used under normal conditions in Eqs. (13) and (14).

Operating reserves such as spinning (provided by online units) and standing (provided by offline units with very fast startup capability) are also considered in the model as shown in Eq. (23) and their net requirements (right hand side of Eq. (23)) are a function of the size of the largest unit and renewable generation (this function will be presented in detail in Section 2.3.4). Eqs. (24)–(26) limit the amount of reserves that can be provided by each generator.

$$\sum_{i \in I^{NR}} R^S_{i,j,s} + FS \cdot \sum_{i \in I^{FS}} (c_i - n_{i,j,s} \cdot \bar{P}_i)$$
$$+ DR^S_{j,s} \geq f\left(\Delta P, \{g_{i,j,s}\}_{i \in I^R}, \{c_i\}_{i \in I^R}\right) \qquad \forall j \in J, s \in S \tag{23}$$

$$R^S_{i,j,s} \leq t^{SR} \cdot n_{i,j,s} \cdot \rho_i \qquad \forall i \in I^{NR}, j \in J, s \in S \tag{24}$$

$$R^P_{i,j,s} + R^S_{i,j,s} \leq n_{i,j,s} \cdot \bar{P}_i - g_{i,j,s} \qquad \forall i \in I^G, j \in J, s \in S \tag{25}$$

$$R^S_{i,j,s} \leq n_{i,j,s} \cdot \bar{P}_i - g_{i,j,s} \qquad \forall i \in I^{NG}, j \in J, s \in S \tag{26}$$

In Eqs. (20)–(23), two types of demand response have been defined, namely $DR^P_{j,s}$ and $DR^S_{j,s}$, and distinction is given by their actions timeframes, e.g. inertial response timeframe (seconds) and operating reserve timeframe (minutes). The same distinction for demand services that can support frequency is found in the Great Britain electricity system as explained in National Grid (2014).

2.3. Assumptions and simplifications

2.3.1. Additional nomenclature

Sets	
I^{GS}:	Set of technologies that participate in primary frequency control and are classified as slow response units for having low emergency ramp rate (subset of I^G).
I^{GF}:	Set of technologies that participate in primary frequency control and are classified as fast response units for having high emergency ramp rate (subset of I^G).

Parameters		
r_t:	Emergency ramp rate of slow ($t = SL$) and fast ($t = FT$) response units.	[MW/s]
H:	Inertia constant of generic unit (any technology).	[s]
$\bar{P}$:	Maximum power output of generic unit (any technology).	[MW]
β_i:	Fraction of generation of renewable technology i to be covered through operating reserve (small-scale study).	[p.u.]

Decision variables		
$n^{min}_{i,j,s}$:	Minimum value between the number of units of technology i under scenario s in hour j, and the number of units of technology i under scenario s in hour j-1.	[−]
$n_{SL,j,s}$:	Number of slow response units that participate in primary frequency control.	[−]
$n_{FT,j,s}$:	Number of fast response units that participate in primary frequency control.	[−]
$n_{NG,j,s}$:	Number of synchronous units that are online and do not participate in primary frequency control.	[−]
$SS_{j,s}$:	Operating reserve requirement at hour j under scenario s in the small-scale study.	[MW]
$LS_{j,s}$:	Operating reserve requirement at hour j under scenario s in the large-scale study.	[MW]
AV_j:	Auxiliary variable used for modeling the operating reserve requirement in hour j.	[MW]

2.3.2. Ramp rate constraints

Constraints (13) and (14) can be represented by using a set of auxiliary variables which are bounded by the numbers of units synchronized of a technology in both period j and j-1. Note that these variables are lower bounded by Eqs. (27) and (28) while are upper bounded by Eqs. (29) and (30). Hence Eqs. (27)–(30) rather than Eqs. (13)–(14) are used in the model. In addition, due to the large size of the model, we neglect constraint (17) which may drive fractional solutions in terms of the number of units synchronized and this is a reasonable simplification since we demonstrate through several experiments that this assumption will not drive a significant MIP gap, e.g. less than 1%.

$$g_{i,j,s} - g_{i,j-1,s} \leq n^{min}_{i,j,s} \cdot \rho_i + (n_{i,j,s} - n_{i,j-1,s}) \cdot \underline{P}_i \qquad \forall i \in I^{NR}, j > 1 \in J, s \in S \tag{27}$$

$$g_{i,j-1,s} - g_{i,j,s} \leq n^{min}_{i,j,s} \cdot \rho_i + (n_{i,j-1,s} - n_{i,j,s}) \cdot \underline{P}_i \qquad \forall i \in I^{NR}, j > 1 \in J, s \in S \tag{28}$$

$$n^{min}_{i,j,s} \leq n_{i,j-1,s} \qquad \forall i \in I^{NR}, j > 1 \in J, s \in S \tag{29}$$

$$n^{min}_{i,j,s} \leq n_{i,j,s} \qquad \forall i \in I^{NR}, j > 1 \in J, s \in S \tag{30}$$

2.3.3. Primary frequency response constraints

Eq. (20) is non-linear but convex and thus can be linearized by using tangent planes. To do so, technologies are grouped into two categories, according to their emergency ramp rates in order to reduce the number of planes and computational resources used. Additionally, a third group is defined which corresponds to technologies that do not participate in PFR but are connected through synchronous machines to the system and thus add inertia to it. Units' contribution to inertia (H) and their maximum power output are assumed to be equal among all units. Hence we re-define the region given by Eq. (20) as that associated with Eqs. (31)–(34). Eq. (34) can be linearized by tangent planes as shown by Fig. 1.

$$n_{SL,j,s} = \sum_{i \in I^{GS}} n_{i,j,s} \qquad \forall j \in J, s \in S \tag{31}$$

$$n_{FT,j,s} = \sum_{i \in I^{GF}} n_{i,j,s} \qquad \forall j \in J, s \in S \tag{32}$$

$$n_{NG,j,s} = \sum_{i \in I^{NG}} n_{i,j,s} \qquad \forall j \in J, s \in S \tag{33}$$

$$\frac{\frac{1}{4}\left(\Delta P - DR^P_{j,s}\right)^2}{\left(1 - \frac{f^{min}}{f^0} - \frac{f^{db}}{f^0}\right)} \leq \left(n_{SL,j,s} \cdot r_{SL} + n_{FT,j,s} \cdot r_{FT}\right)$$
$$\cdot \left((n_{NG,j,s} + n_{FT,j,s} + n_{SL,j,s}) \cdot H \cdot \bar{P} - H_f \cdot \Delta P\right) \qquad \forall j \in J, s \in S \tag{34}$$

Additionally, Eq. (22) is non-convex and thus we define two alternative convex LP models that serve as upper and lower bounds to the optimal solution. The lower bound is obtained by removing Eq. (22) from the formulation, leading to a portfolio solution with a lower expected cost of investment and operation but which may violate Eq. (22) and thus be technically infeasible. The upper bound solution is obtained by fixing participation of certain technologies for the provision of PFR services according to historical engineering practices. We may produce several upper bound solutions by defining various levels of participation from different generation technologies in PFR. Hence, a number of technically feasible suboptimal solutions can be obtained, ultimately selecting that with the lowest gap with respect to the lower bound solution. We found for all case studies analyzed
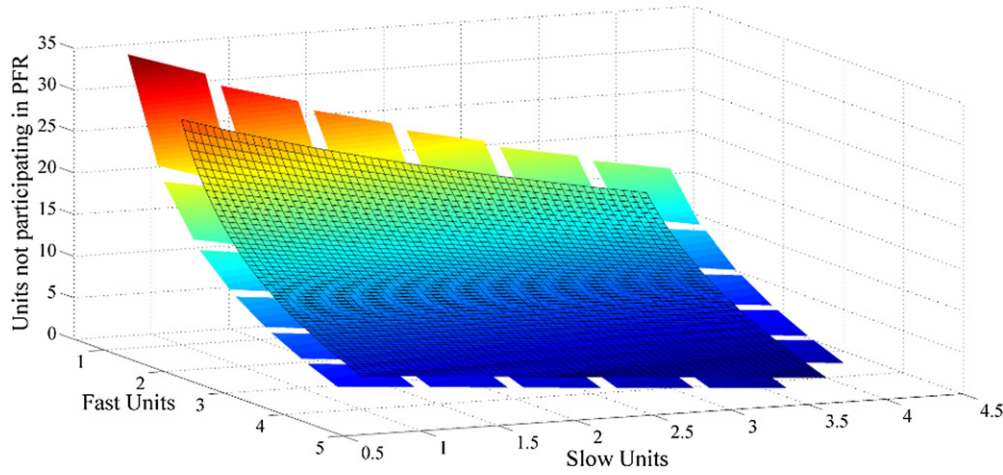
Fig. 1. Linearization of Eq. (34) through tangent planes.

in this paper that the selected technically feasible solutions present less than 0.8% gap.

2.3.4. Operating reserves constraints

We use two criteria to define the amount of necessary operating reserves in Eq. (23), where the main difference lies in the treatment of uncertainty associated with renewable generation outputs in operational timescales. According to the simplest criterion, operating reserves are held by the system operator proportionally to the amount of renewable generation dispatched and this is used for fundamental studies. Specifically, Eqs. (35)–(37) show that the amount of reserve has to be the largest between requirements for renewables and those to deal with the outage of the largest unit and this is according to reference Silva (2010). In consequence, when no renewable generation is dispatched, the N-1 criterion is still met.

$$\sum_{i \in I^{NR}} R^S_{i,j,s} + \text{FS} \cdot \sum_{i \in I^{FS}} \left(c_i - n_{i,j,s} \cdot \overline{P}_i\right) + \text{DR}^S_{j,s} \geq SS_{j,s} \qquad \forall j \in J, s \in S \tag{35}$$

$$SS_{j,s} \geq \sum_{i \in I^R} \beta_i \cdot g_{i,j,s} \qquad \forall j \in J, s \in S \tag{36}$$

$$SS_{j,s} \geq \Delta P \qquad \forall j \in J, s \in S \tag{37}$$

We used a more realistic criterion for the representation of operating reserve policies, where reserve amounts required (*Req*) are dependent on the forecast errors of renewable generation as shown in Eq. (38) and defined in reference Silva (2010), and this is used in our paper for large-scale studies.

$$\text{Req} = \Delta P + 3 \cdot \sqrt{\sigma^2_{\text{WIND}} + \sigma^2_{\text{SOLAR}}} \tag{38}$$

Standard deviations of wind and solar forecast errors shown in Eq. (38) – σ_{WIND} and σ_{SOLAR}, respectively – have to be computed using a certain forecast policy. As wind speed and solar radiation are different phenomena, their forecast techniques to predict future generation output differ. Hence we use persistent forecast for wind according to Silva (2010), Strbac et al. (2006) while a more time dependent forecast method is used for solar power. Eq. (38) can be written as a function of renewables' installed capacity and this is shown in Eq. (39) which also considers lower volumes of reserve for those periods where wind does not present a significant power production

and this is according to actual practices by system operators as explained in Silva (2010).

$$f\left(\Delta P, \left\{g_{i,j,s}\right\}_{i \in I^R}, \left\{c_i\right\}_{i \in I^R}\right) \tag{39}$$

$$= \begin{cases} \Delta P + 3 \cdot \sqrt{c^2_{\text{WND}} \cdot \sigma^2_{\text{WND}} + c^2_{\text{SOL}} \cdot \sigma^2_{\text{SOL},j}} & RP_{\text{WND},j} \geq 3 \cdot \sigma_{\text{WND}} \\ \Delta P + g_{\text{WND},j,s} + 3 \cdot c_{\text{SOL}} \cdot \sigma_{\text{SOL},j} & RP_{\text{WND},j} < 3 \cdot \sigma_{\text{WND}} \end{cases}$$

As Eq. (39) is non-linear, we use the approximation shown by Eqs. (40)–(43). Fig. 2 illustrates how the approximation works.

$$\sum_{i \in I^{NR}} R^S_{i,j,s} + \text{FS} \cdot \sum_{i \in I^{FS}} \left(c_i - n_{i,j,s} \cdot \overline{P}_i\right) + \text{DR}^S_{j,s} \geq LS_{j,s} \qquad \forall j \in J, s \in S \tag{40}$$

$$LS_{j,s} = \begin{cases} \Delta P + 3 \cdot \left(\frac{1}{\sqrt{2}} \cdot \left(c_{\text{WND}} \cdot \sigma_{\text{WND}} + c_{\text{SOL}} \cdot \sigma_{\text{SOL},j}\right) + \left(1 - \frac{1}{\sqrt{2}}\right) \cdot AV_j\right) & RP_{\text{WND},j} \geq 3 \cdot \sigma_{\text{WND}} \\ \Delta P + g_{\text{WND},j,s} + 3 \cdot c_{\text{SOL}} \cdot \sigma_{\text{SOL},j} & RP_{\text{WND},j} < 3 \cdot \sigma_{\text{WND}} \end{cases}$$

$$\forall j \in J, s \in S \tag{41}$$

$$AV_j \geq c_{\text{WND}} \cdot \sigma_{\text{WND}} - c_{\text{SOL}} \cdot \sigma_{\text{SOL},j} \qquad \forall j \in J \tag{42}$$

$$AV_j \geq -\left(c_{\text{WND}} \cdot \sigma_{\text{WND}} - c_{\text{SOL}} \cdot \sigma_{\text{SOL},j}\right) \qquad \forall j \in J \tag{43}$$

3. Small-scale study

The small-case example will be used to illustrate the proposed cost-risk model that serves to find the optimum portfolio of generation technologies, including renewables. Hence the efficient cost-risk Pareto
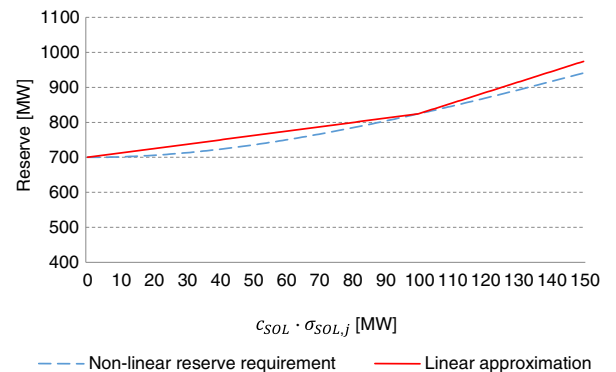

Fig. 2. Linear approximation of Eq. (39) for $RP_{\text{WND},j} \geq 3 \cdot \sigma_{\text{WND}}$ and $c_{\text{WND}} \cdot \sigma_{\text{WND},j} = 100$ [*MW*].
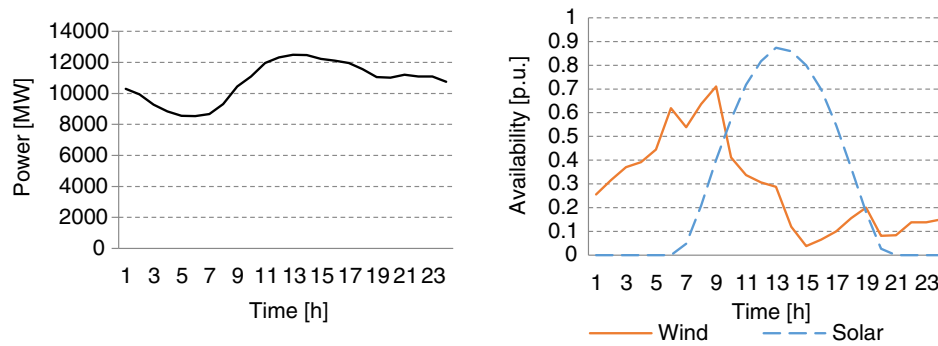
Fig. 3. (a) Demand (left) and (b) renewable generation profiles (right).

boundary of generation portfolios is determined and compared to those obtained by alternative methods, highlighting the effects of system security on optimum portfolio selection. In addition, we study the effects of demand services on accommodating renewables' generation outputs and thus on supporting investment in technologies such as wind and solar power.

In this context, the case study in this section is simplified through a small set of scenarios, generation technologies, number of hours, etc., for the sake of simplicity and clarity. Thus, the numerical results shown in this section (e.g. average indicators such as the expected costs of generation, risk indicators such as CVaR) are illustrative (rather than realistic) and should be interpreted with care. Section 4, on the other hand, presents a realistic exercise applied to the Chilean generation sector, which serves to demonstrate the full capabilities of the proposed modeling framework.

3.1. Input data

In this small-scale case study we consider 5 generation technologies, namely coal, oil, hydro (reservoir), wind and solar. Annuitized investment costs used are 200 $/kW-year (~2000 $/kW as upfront capital cost, assuming 10% real discount rate) for coal, reservoir and wind generation technologies, 50 $/kW-year (~500 $/kW) for oil plants, and 250 $/kW-year (~2700 $/kW) for solar plants. We assume that coal and oil generation technologies' variable costs present an expected value of 50 and 150 $/MWh, respectively, and a standard deviation of 12.5 and 45 $/MWh, respectively, following normal distributions which are perfectly correlated. These scenarios represent uncertainty in fossil fuel prices which is combined with uncertainty in hydrological conditions (inflows) that significantly affect the annual cost of system operation. Hence we build 120 scenarios that represent combination of 40 potential realizations of variable costs with 3 hydrological (inflow) scenarios that represent load factors of 20%, 40% and 60% for hydro plants. A value of lost load (VoLL) equal to 400 $/MWh is used and this is according to the regulation of the power sector in Chile. Demand, wind and solar profiles used are shown in Fig. 3 that present an average load factor 86%, 29% and 30%, respectively, where the optimization horizon covers 24 hours.

Minimum and maximum units' outputs are assumed to be 50 and 400 MW with an hourly ramp rate (ρ_i) of 100 MW/h for coal and 350 MW/h for all other conventional technologies. Emergency ramp rates (r_i) are those used by Chávez and Baldick (2012) and equal to 38 MW/s for thermal plants and 8 MW/s for hydro plants. In real power systems, primary frequency response service is provided by a subset of the conventional plants synchronized, which is represented in our model by defining two types of units per technology: with and without capability to respond to frequency changes in which the former presents a slightly higher investment cost that allows us to quantify the demand for the frequency response service. Also, operation is secured against the outage of a single unit (i.e. 400 MW) under which frequency

is not allowed to violate a minimum value of 49.2[1] Hz from a nominal value of 50 Hz (governors' dead-band are assumed to be equal to ± 25[2] mHz and units' inertia (H) is equal to 5 s). Regarding operating reserves needed for renewables, we assume that they should be sufficient to cover variations up to 45% of their net output ($\beta_{WND} = \beta_{SOL} = 45\%$). This is a simplification used to study the fundamentals of cost-risk generation planning with security and we use a more realistic demand function for operating reserves in our next large-scale example.

Finally, we assume that costs associated with demand services are equal to zero (in order to study its benefits), reservoir seepage and evaporation losses are equal to 0.5% of stored water, and maximum capacity of the reservoir is very high and thus does not constrain hydros' output. Portfolios will be determined by using an α-CVaR with an α of 95%.

3.2. Cost-minimizing and risk-averse investment decisions

Cost expectations are minimized when no risk constraint is imposed which leads to a generation technology portfolio composed of coal and hydro plants. These technologies are less costly in average terms and thus are preferred under a minimum cost framework. However, if the exposure of the selected generation portfolio to risks is constrained, investment in conventional technologies may be partially displaced by contribution from renewable generation and this is illustrated in Fig. 4 and Table 1 that present the cost-risk Pareto boundary and its corresponding investment decisions.

Table 1 shows that there is a clear tendency to reduce participation of hydropower generation as risk exposure is minimized. Although hydro plants are the most economic investment option and therefore preferred in the minimum cost solution, it drives risk exposure due to uncertainty in hydro production. In fact, we assume that in a dry year hydro plants can produce only at 20% load factor while in a wet year production increases up to 60% load factor. Since lack of hydro production that can occur in dry years can significantly increase the cost of operation in a system with high penetration of hydro (including cost of unsupplied demand), hydro share is reduced in risk-averse portfolio selections.

In contrast, penetration of coal generation does not present a monotonic trend with respect to risk levels as that of hydro. In fact, coal generation increases in risk-averse portfolio selections when no renewables are built, and decreases otherwise. This is so since, on the one hand, risk caused by uncertain hydrological conditions can be hedged by a higher share of coal generation and, on the other hand, a significant penetration of coal may cause exposure to further risks such as that associated with fuel costs. Hence an optimum cost-risk portfolio selection will

---

[1] Chilean regulator states that under frequency load shedding must take place when system frequency reaches a threshold of 49.2 Hz (National Energy Commission, 2014b).
[2] Maximum allowed governors' dead band in Chile (National Energy Commission, 2014b).
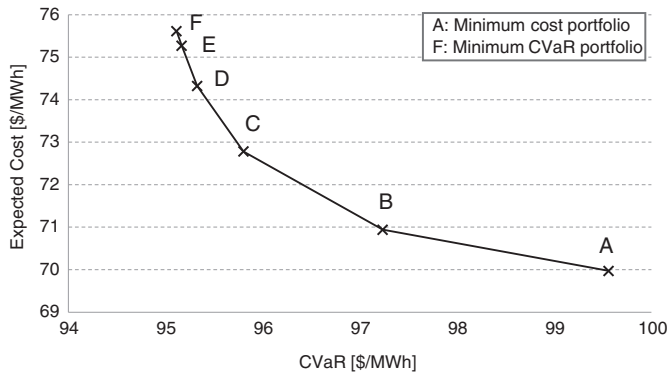
Fig. 4. Cost-risk Pareto boundary.

Table 1
Optimum generation portfolios.

	A	B	C	D	E	F
Installed capacity [MW]						
Wind	0	0	2917	4590	5049	5060
Solar	0	0	0	1024	1890	2248
Coal	7174	8342	8537	8171	8022	8018
Reservoir	17,936	12,139	8829	7680	6886	6459
Oil	0	0	0	0	0	0
Expected generated energy						
Wind	0%	0%	8%	12%	13%	14%
Solar	0%	0%	0%	3%	5%	6%
Coal	33%	55%	59%	56%	56%	56%
Reservoir	67%	45%	33%	29%	25%	24%
Oil	0%	0%	0%	0%	0%	0%
Expected cost [$/MWh]	70	70.9	72.8	74.3	75.3	75.6
CVaR [$/MWh]	99.6	97.2	95.8	95.3	95.2	95.1

hedge hydrological risks by installing thermal generation first, and use renewables as a second and more expensive option to reduce risks further as shown in Table 1.

In this context, Fig. 5 shows that although risk exposure to fossil fuel prices and hydrological conditions can be handled by an optimum combination of thermal and hydro generation, it can be further reduced and efficiently minimized by building renewable generation.

From Fig. 5 it can also be concluded that if hydrological risk is not properly considered in the portfolio analysis, the value of renewables may be under-estimated and in consequence, less risk mitigating renewable generation capacity may be built. As previous research demonstrates (see, for instance, references Awerbuch (2006), Bazilian and Roques (2008), Roques et al. (2008)), in portfolio theory the investment decision in new installed capacity depends not only on the stand-alone cost-risk profile of the new alternatives but also on the current generation mix that the system presents.

Both wind and solar plants are used to reduce risks albeit we have assumed that solar is significantly more expensive in terms of its unit cost (i.e. 78.7[3] $/MWh of wind against 95.1 $/MWh of solar). Through various sensitivity analyses where demand profiles and solar availability and cost are changed, we demonstrate that investment levels observed in solar plants are mainly justified by the high correlation between solar and demand profiles. Furthermore, as hydro is essentially a technology that produces at peak demands, reduction in hydro capacity investment caused by significantly contained risk levels, drives investment in solar that can do both: produce at peak demands and displace investment in peaking plants such as oil that would escalate portfolios' cost and risk.

Note that the VoLL used in our study corresponds to levels observed in a developing country's electricity system and thus this may be considered small with respect to levels observed in developed countries. Hence we carried out a sensitivity analysis for higher VoLL and observed that the efficient portfolios remained unchanged since the current solutions (shown above) already eliminated the load curtailed (i.e. although VoLL used may be considered small, it is sufficiently high with respect to alternative costs of building and operating generation assets).

Our previous results are in line with published studies such as that in references Bazilian and Roques (2008), Roques et al. (2008), where the hedging effects of renewables against fuel prices were studied in extent. In this context, our framework expands on the previous findings and demonstrates for the first time how investment in hydropower can be coordinated with further renewable and non-renewable generation capacity investment within a cost-risk optimization framework, complementing the previous research that mainly focused on thermal systems.

---

[3] Calculated using: $INV_{i,s}/(8760 \cdot \overline{lf})$, $\overline{lf}$ = Average load factor.

3.3. Effects of security of supply on optimum portfolio selection

Through constraints (20)–(26), our method ensures that optimum portfolio of generation technologies built can be operated securely, recognizing the costs of various services to maintain system frequency stability. Hence we compare solutions from purely economic cost-risk models like that developed by Delarue et al. (2011) against solutions from our model that considers the costs associated with secure operation. Fig. 6 shows that although purely economic models seem to present a more efficient cost-risk Pareto boundary (Unsecure Planning/Unsecure Operation) than those obtained by our model (Secure Planning/Secure Operation); the former ignores costs associated with security of supply. In fact, if investment solutions obtained by models that ignore the need for reserves are operated in a secure fashion (as any system operator would utilize new generation infrastructure), real costs and risks of investment will be much higher than those initially estimated (Unsecure Planning/Secure Operation).

Furthermore, if the need for security is ignored, higher volumes of investment in renewables will be promoted that will lead to either higher cost to secure system operation or very low levels of security of supply in operational timescales since resources that provide such security were not properly planned. This can be observed in Fig. 7 that shows the operation of the minimum risk solution obtained by a purely economic model (under a particular scenario) in two modes: with consideration of security of supply and without it. Hence if the generation infrastructure determined is forced to operate securely as shown in Fig. 7(b), demand would be curtailed in the evening since hydro power needs to be used along the day to provide frequency control services, which is ignored in Fig. 7(a). In this case, frequency control services could not be efficiently provided without hydro plants due to the
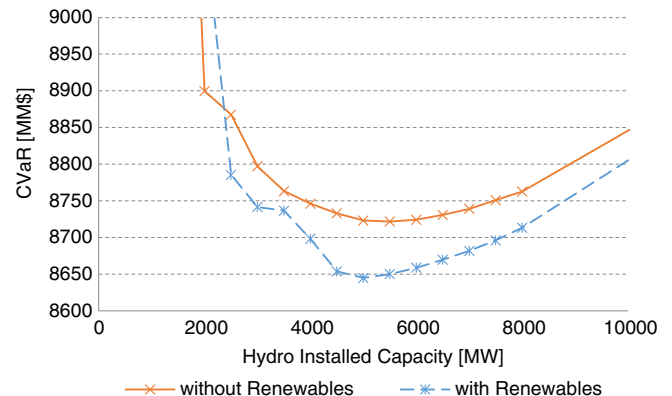

Fig. 5. CVaR versus hydro (reservoir) installed capacity with and without renewables.
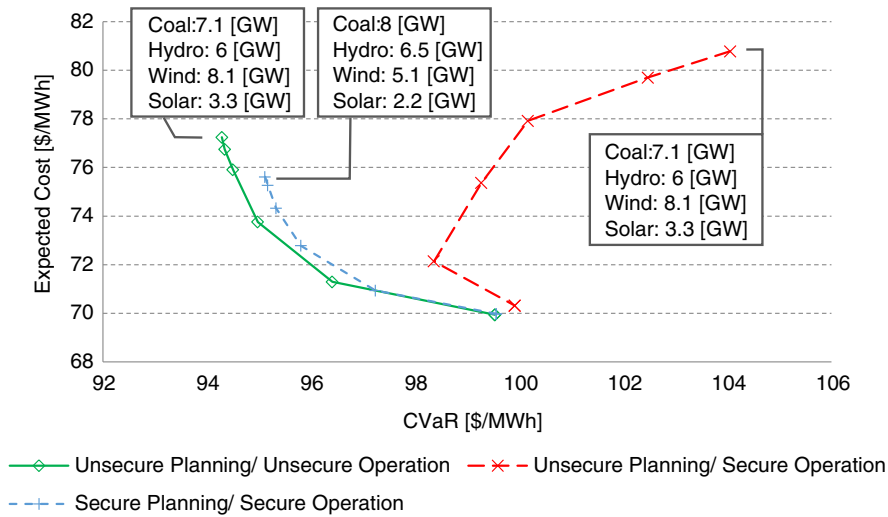
Fig. 6. Cost-risk Pareto boundaries comparison of generation portfolios with and without security of supply.

limited ability of other technologies to ramp and contribute to operating reserves. In addition, solar power plants are curtailed since system capability to absorb renewable generation is also limited.

Various analyses of the dual prices associated with constraint (20) also demonstrate the importance of security. For example, we observed that if system inertia is compromised by high levels of wind or solar outputs, our model will schedule out-of-merit generation in order to: (i) synchronize a higher number of partially loaded economic plants and thus increase system inertia; (ii) synchronize units that can provide very fast frequency response service and thus improve system's capability to ramp under emergency conditions; and (iii) curtail renewables output if the above-mentioned measures do not suffice to maintain minimum frequency drop under certain levels. In Fig. 7(b), operational measures to maintain acceptable levels of frequency drops are needed in hour number 3 and 23.

3.4. Effects of demand services on cost, risk and generation portfolio selection

In the above case studies, demand actions to either secure portfolio selections (through demand response) or make them more economically efficient (through demand shift), are neglected. Thus, we analyze next the contribution from demand flexibility to economics and security performance of both system operation and planning. Demand flexibility may be enabled by smart grid solutions that can control, for example, thermal loads in real time (Papadaskalopoulos et al., 2013).

3.4.1. The role of demand response

Demand response refers to the ability to reduce load in a timely fashion in order to control frequency after an outage occurs. Fig. 8 shows various cost-risk Pareto boundaries for different levels of demand response. Interestingly, demand response improves the Pareto boundary, presenting a larger impact on those portfolios with limited risk exposure while no effect is observed on those solutions that minimize cost expectation. This is so since security constraints are not critical on those cases without a significant amount of renewables. In fact, when all units are synchronous in the operation, system inertia is robust, and amount and cost of response and reserves are minimal. Fig. 8 also shows that demand response can increase participation of renewables in generation portfolios since cost of security needed to maintain system stable with high renewables output can be reduced by utilization of demand control.

3.4.2. The role of demand shift

Demand shift refers to the ability to reduce load during peak demand conditions and increase load during off-peak periods in order to balance overall energy consumption within a day and improve system's economic performance. Fig. 9 shows various cost-risk Pareto boundaries for different levels of demand shift capability, and demonstrates similarly to demand response, improvement of cost-risk Pareto boundary while increasing demand shifted volumes, especially in portfolios with reduced risk levels with higher participation of renewables. For the risk-neutral portfolio, effect of demand shift is negligible since hydro generation can provide enough flexibility (by prioritizing production
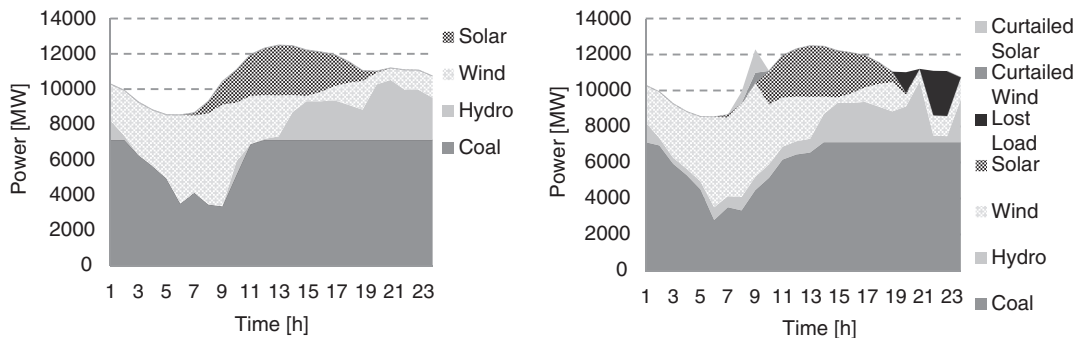

Fig. 7. (a) Underlying operation of generation portfolio obtained without security considerations (left), and (b) secured operation of generation portfolio obtained without security considerations (right).
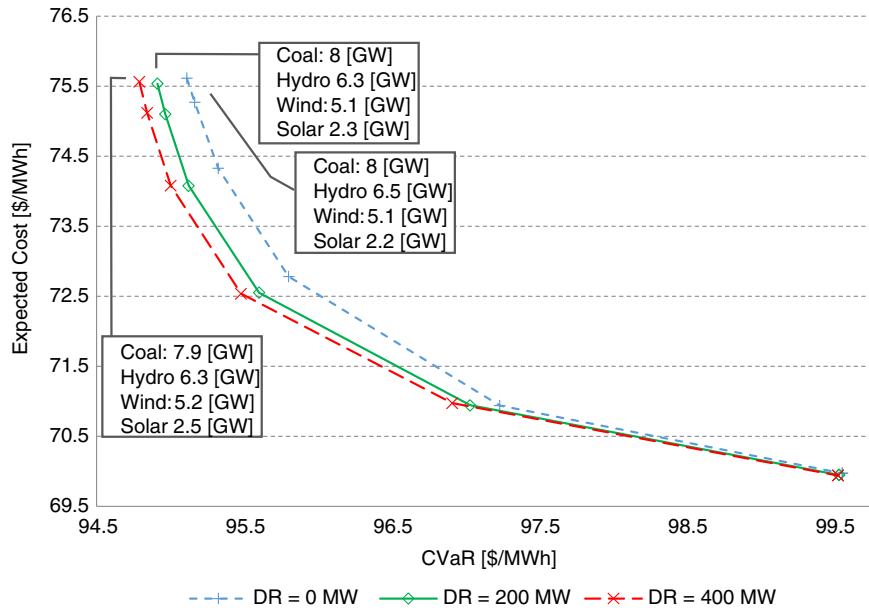
Fig. 8. Cost-risk Pareto boundaries (demand response sensitivity).

during peaks) to improve efficiency of thermal plants. As risk-averse investment decisions seek the correct balance between renewable and hydro generation, demand shift can provide required levels of flexibility to increase penetration of renewables and reduce share of hydro plants and this is also shown in Fig. 9. Note that demand shift modeling can also be used to study effects of energy storage plants (e.g. battery, hydro pumped storage, etc.) on planned generation portfolios.

4. Large-scale study

The large-scale study will be used to obtain results and insights over a more realistic case that represents the main Chilean electricity system for which minimum cost and risk generation portfolios are determined. Given the very large volumes of data that have to be considered in the optimization (1000 scenarios that combined multiple fuel costs and hydrological conditions across 8760 hours), we use a Benders decomposition-based algorithm in a parallel computing fashion and

demonstrate its ability to tackle large-scale problems. This algorithm is detailed in the Mathematical Appendix.

We implemented our method in FICO suite optimization (FICO, 2014) by using a computer with 192 GB of RAM and 2 Intel Xeon X5690 (3.46 GHz) processors.

4.1. Generation input data

We divided generation units into 7 technologies as shown in Table 2 that also presents operating and investment costs together with technologies' lifespans, current installed capacity and total potential. Data are according to the average values observed in Chile (National Energy Commission, 2014a, 2016; Ministry of Energy, 2015) and the U.S. Energy Information Administration (EIA, 2015). Investment costs were annuitized using a 10% real discount rate.

Reserve requirements are those according to Eqs. (40)–(43) with a standard deviation equal to 12.8% during all hours for wind output
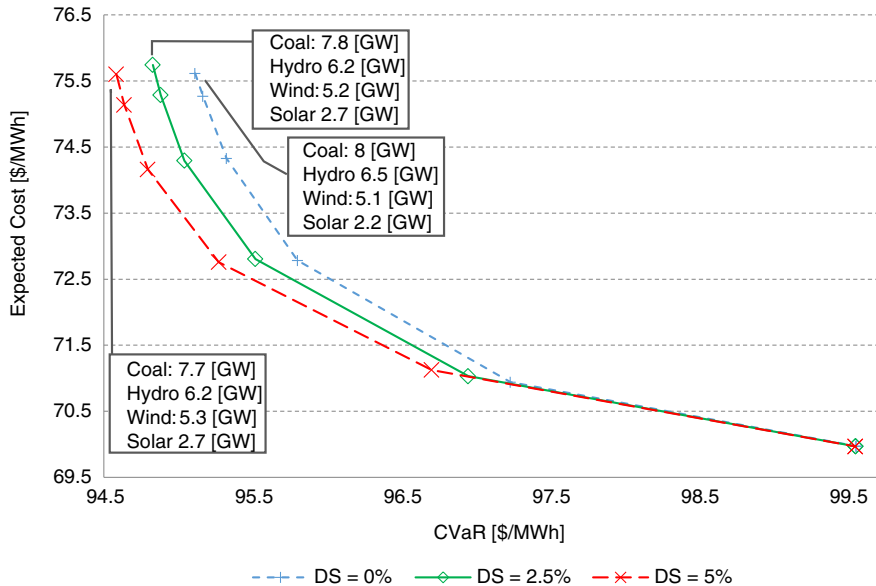

Fig. 9. Cost-risk Pareto boundaries (demand shift sensitivity).

Table 2
Generation input data.

	Investment cost	Fixed maintenance cost	Variable maintenance cost	Lifespan	Current installed capacity	Resource potential
	[$/kW]	[$/kW-year]	[$/MWh]	[years]	[MW]	[MW]
Wind	1491	40	-	20	810	-
Solar	1690	25	-	25	443	-
Coal	2727	31	5	24	2170	-
Reservoir	2900	15	-	50	3393	6200
Oil	500	7	10	24	2591	-
LNG	1053	13	4	24	2543	-
Run-of-river	2900	15	-	50	2615	6200

forecast errors, and with a standard deviation equal to 0% to 10.6% depending on the particular hour of the day for solar output forecast errors. Hourly demand profile is that of 2012 which was scaled up in order to meet 2025 projections undertaken by the Chilean regulator (peak of 12.5 GW and energy consumption of 87.1 TWh).

Each aggregated wind and solar generation profile was determined from real measurements across expected placement of future generation and can be found in references University of Chile, 2014a; University of Chile, 2014b. These profiles present average load factors of 28% and 24% for wind and solar generation, respectively.

Minimum outputs of units that provide frequency control services are assumed to be 40% of the maximum output for thermal units (160 MW) and 10% for hydro power units (40 MW). Ramp rates for the hourly commitment of units (ρ_i) are considered to be 10% of the maximum output for coal units, 50% for LNG units and 100% for remaining technologies.

Regarding hydro plants, one representative reservoir is considered and we assume that the average inflow-to-power rate is equal to 1.9 MW/m³/s, lower and upper bounds for the stored water ($\underline{v}_i$ and $\overline{v}_i$) are equal to[4] 1,556 hm³ and 10,321 hm³, respectively, and losses due to evaporation and seepage (λ_i) are equal to 0.002% of the stored water level in each hour. Data associated with reservoirs were obtained from the actual software used by the system operator to run the Chilean system.

Finally, value of lost load (*voll*), emergency ramp rates (r_t), maximum output of units ($\overline{P}$), size of largest generation outage (ΔP), frequency dead-band of governors (f^{db}), minimum frequency allowed under contingency (f^{min}), nominal frequency (f^0), inertia of units (H), deployment time of operating reserves (t^{SR}), demand shift costs (dc^- and dc^+) and the α parameter for the α-CVaR measure are those of the small-scale example analyzed in the previous section.

4.2. Scenario modeling

Hydrological and fossil fuel price scenarios are combined in order to represent uncertainty through 1000 scenarios as explained next.

4.2.1. Fossil fuel price scenarios

Previous works such as those of references Jansen et al. (2006), Doherty et al. (2006), Delarue et al. (2011), Sunderkötter and Weber (2012) use variance as the risk measure and thus Gaussian distributions are suitable to represent uncertainty of fossil fuel prices. As we used a scenario-based approach and a CVaR risk measure, a proper random walk process can be used to represent uncertainty in future prices and thus fossil fuel prices are assumed to follow a correlated, geometric Brownian motion which is a standard assumption in finance as explained in Hull (2009). Hence through a Monte-Carlo process we

can use Eq. (44) to generate prices in a given year.

$$P^i_{t+\Delta t} = P^i_t \cdot e^{\left(\mu_i - \frac{1}{2}\sigma_i{}^2\right)\cdot \Delta t + a_i \cdot \sqrt{\Delta t}} \tag{44}$$

Where μ_i and σ_i are the mean and standard deviation of year-to-year fossil fuel prices returns and a_i is the ith component of the vector resulting from the multiplication $\boldsymbol{C} \cdot \boldsymbol{\epsilon}$, where $\boldsymbol{C}$ is the Cholesky decomposition matrix of the Variance–Covariance matrix $\sum$ (i.e. $\boldsymbol{\Sigma} = \boldsymbol{C} \cdot \boldsymbol{C^T}$) and $\boldsymbol{\epsilon}$ is a vector with random values that distributes $N(0,1)$. Δt represents the time lag between the moment when the investment decision is made and a given year in the future.

Time series of fossil fuel prices were obtained from the U.S. Energy Information Administration (EIA, 2014a, 2014b, 2014c). Table 3 shows the statistical parameters of the time series used.

A 6-year lag is assumed ($\Delta t = 6$), which represents an average construction time in Chile. As the target year is 2025, prices envisaged by regulator for 2019 were used as initial prices (P^i_t). Expected returns of fuel prices (μ_i) were assumed equal to the 6-years[5] real yield of bonds issued by the Chilean government which is approximately 2% and this is according to Hull (2009), Gorton et al. (2013).[6]

Finally, the statistical data of the generated (log-normal) distributions for the fossil fuel prices are shown in Table 4 and used to elaborate 100 Monte-Carlo fossil fuel scenarios.

4.2.2. Hydrological scenarios

By using real data provided by the system operator, 10 hydrological scenarios were produced which are considered to represent the range of inflows observed over the last 50 years. Probabilities and average load factors of profiles associated with inflows of run-of-river and reservoir generation are shown in Table 5.

In our model, uncertainties associated with different hydrological scenarios that can occur are considered only in planning timescales for investment decisions. Hence uncertainty in availability of hydro resources for short-term operation is not modeled and this is a common assumption in this type of studies as explained in Unsihuay-Vila et al. (2010) since the focus is on system planning.

4.3. Results and discussion

Table 6 shows our results for the minimum cost and risk generation portfolios in which 5% of hourly demand can be shifted and 200 MW of demand response can be utilized to provide frequency control services. Similarly to our results in the previous sections, investment in reservoir hydro plants is limited when a more risk-averse solution is preferred; nevertheless, the model ensures that flexibility of the generation mix is still sufficient to deal (in operational timescales) with the uncertainty and (hourly) intermittency associated with the new investment in

---

[4] As the model considers upper and lower bounds of the representative reservoir to be proportional to the installed capacity, these values correspond to the case when the installed capacity of the reservoir is equal to the minimum installable capacity (3393 MW).

[5] Since Chilean bonds are issued for maturities of 5 and 10 years, linear interpolation was done to calculate the 6-year real yield.

[6] Empirical studies generally find the systematic risk of commodity futures to be close to zero and fail to reject a non-zero risk premium for individual commodity futures (see Bessembinder (1992), Kolb (1992), Erb and Campbell (2006)).

Table 3
Statistical data of fuel price returns' time series.

	Coal	LNG	Oil
Mean	2%	2%	6%
Standard deviation	12%	14%	21%

Correlation coefficients	Coal	LNG	Oil
Coal	1	-	-
LNG	0.4	1	-
Oil	0.2	0.7	1

Table 4
2019 Expected fuel prices and 2025 fuel price distributions.

	Coal	LNG	Oil
Base price (2019) [$/MWh] ($P^i_t$)	38	95	184
Expected price (2025) [$/MWh]	43	107	204
Standard deviation (2025) [$/MWh]	14	37	117
Coefficient of variation	31%	35%	58%

Table 6
Optimum 2025 generation portfolios.

	Minimum cost		Minimum risk	
	Installed capacity [MW]	Expected generation	Installed capacity [MW]	Expected generation
Wind	4586	13.00%	6736	19.05%
Solar	443	1.08%	3640	8.88%
Coal	2790	24.00%	3912	24.58%
Reservoir	5654	24.71%	3393	14.87%
Oil	2591	0.38%	2591	0.04%
LNG	2543	4.60%	2543	0.42%
Run-of-river	6200	32.25%	6200	32.17%
Expected cost [$/MWh]	81.72		85.65	
CVaR [$/MWh]	111.30		100.12	

renewables. Interestingly, investment in renewables will be accompanied by higher investment levels in coal plants which are found to be less risky than reservoir power plants (note that we have not considered carbon taxes in this study). Potential of run-of-river plants, on the other hand, is always fully used since it reduces exposure to fuel price volatility and their inflows appear to be steadier within the different scenarios, in comparison to other hydro technologies. Investment in wind rather than solar is encouraged in the minimum cost solution while the value of solar power is clearly disclosed in the risk-averse solution, where a more balanced wind/solar portfolio is chosen as an optimal hedge against risks in fossil fuel prices and inflows. Finally, new investments in oil and LNG are not promoted under any circumstance. Although energy production from oil plants is minimized, their capacity is needed to provide standing reserve services.

In light of these results, we can conclude that by 2025 up to about 28% of demand can be produced from wind and solar in an economically efficient fashion with generation portfolios that can properly hedge uncertainties associated with fossil fuel prices and hydrological conditions. This penetration level can also be efficiently handled from a system security point of view by system operators and in fact wind penetration has been already reduced by a factor of 0.71 due to security constraints (with respect to a case without security constraints). Note that this level of renewables penetration is economically efficient from a cost-risk perspective and without environmental considerations. Hence, further investment in wind and solar may be justified by taking account of environmental costs (e.g. emission costs that penalize production from conventional generation) and further flexibility provision from demand and storage. Also, if investment costs of wind and solar generation are reduced, further investment can be encouraged in these technologies, displacing coal generation capacity of the above portfolios. Under this investment cost sensitivity, we also observed that the high share of run-of-river plants remains the same, which demonstrates the robustness and efficiency levels of investment decisions in run-of-river units.

5. Conclusions and further work

We contribute with a LP cost-risk optimization model to determine efficient generation technology portfolios, which can properly balance the benefits of energy source diversification and cost of security of supply through the provision of various generation frequency control and demand side services, including preservation of system inertia levels. The model can determine risks from scenarios rather than from standard deviations of simplified Gaussian distributions, and tackle a large input data set through an efficient Benders-based method. All these make the model more applicable and suitable for real policy and planning studies.

Through several studies we demonstrate the importance of renewables in hedging both fossil fuel and hydrological risks and confirm that approaches which neglect risk will significantly undermine the value of renewables to diversify energy sources. We also demonstrate that properly accounting for hydrological risk, is paramount to correctly assess the value of renewables, especially in reducing cost spikes during dry seasons. Additionally, we show the effect of security of supply on increasing costs and risks, and constraining renewables investment. In this context, we highlight the importance of demand side actions which can encourage higher volumes of investment in risk mitigating renewable generation capacity. Finally, scalability of our model was proved by running a case study on the Chilean main electricity system in which planned generation infrastructure was run over 8760 hours in 1000 scenarios. In this particular case, we demonstrate the economic benefits associated with investment in wind, solar and run-of-river generation (that can take the form of small hydro units) for the Chilean electricity sector by 2025.

These types of analyses can be particularly interesting for policy makers and regulators that seek cost-effective integration of different renewable generation technologies in both thermal and hydrothermal systems. Our analysis is especially useful in hydrothermal systems either with or without new envisaged developments in hydropower generation since, from a portfolio analysis perspective, investment decisions significantly depend on the existing generation mix (that can present important volumes of hydro capacity). Hence if new hydro plants are envisaged to be developed (as it may be the case in countries such as Russia, China, Canada, Brazil that present large levels

Table 5
Hydrological scenarios.

	H1	H2	H3	H4	H5	H6	H7	H8	H9	H10
Probability [p.u.]	0.06	0.06	0.13	0.17	0.13	0.11	0.17	0.08	0.04	0.06
Reservoir equivalent average capacity factor	16%	24%	30%	34%	41%	46%	52%	57%	63%	71%
Run-of-river average capacity factor	42%	49%	51%	47%	51%	53%	55%	58%	54%	59%

of unexploited potential (World Energy Council, 2015)), our model will properly capture both hydrological and fossil-fuel price risks in investment decisions that include the presence of new hydro plants. In contrast, if no (or small capacity of) hydro plants are envisaged to be developed (as it may be the case in jurisdictions such as Mexico, Norway, Italy or Switzerland that present large levels of their potential already exploited (International Energy Agency, 2010)), our model will properly capture the benefits of new renewables such as wind and solar in hedging both existing levels of hydrological risks and fossil-fuel price risks. Moreover, the proposed framework can also be interesting for policy makers and regulators to (i) justify renewable generation investment in the absence of formal renewables targets, (ii) adjust/improve existing mechanisms that encourage integration of renewables (e.g. renewable portfolio standards) in order to increase the efficiency levels of new investment, and (iii) analyze alternative regulatory frameworks aimed at mitigating risks in future generation investment decisions and these topics are suggested for future research.

Acknowledgments

Mathematical Appendix. Benders decomposition-based algorithm

In this section the Benders decomposition-based algorithm used for tackling large-scale problems is described. The master and slave problems make investment and dispatch decisions, respectively. Investment decisions made in the first stage attempt to minimize total cost of investment and operation across a large number of future scenarios subject to a given level of CVaR associated with these costs. In the master problem, operation costs are represented through a convex function of the investment as shown in Eqs. (A.1)–(A.4) and thus operation variables such as generators' outputs are not explicitly considered.

$$(P1) \, Minimize \, z = \boldsymbol{d}^{\mathrm{T}} \cdot \boldsymbol{y} + \sum_{s \in S} p_s \cdot \mathrm{Q}(\boldsymbol{y}, \boldsymbol{c_s}, \boldsymbol{F_s}) \tag{A.1}$$

s.t.:

$$\delta + \frac{1}{1-\alpha} \cdot \sum_{s \in S} p_s \cdot \left(\boldsymbol{d}^{\mathrm{T}} \cdot \boldsymbol{y} + \mathrm{Q}(\boldsymbol{y}, \boldsymbol{c_s}, \boldsymbol{F_s}) - \delta \right)^+ \leq \overline{\mathrm{CVaR}} \tag{A.2}$$

$$\boldsymbol{y} \in \boldsymbol{Y} \tag{A.3}$$

$$\delta \geq 0 \tag{A.4}$$

In Eqs. (A.1)–(A.4), $\boldsymbol{Y}$ is a set of polyhedral constraints, $\boldsymbol{y}$ is the set of first-stage decision variables (investment) and $\boldsymbol{d}$ is a vector containing investment costs. Also, $(x)^+ = \max(x, 0)$ and $\overline{CVaR}$ is the maximum allowed portfolio's CVaR.

The second-stage problem (operation) is given by:

$$(P2_s) \, \mathrm{Q}(\boldsymbol{y}, \boldsymbol{c_s}, \boldsymbol{F_s}) = Minimize \, \boldsymbol{c_s}^{\mathrm{T}} \cdot \boldsymbol{x} \tag{A.5}$$

s.t.:

$$\boldsymbol{F_s} \cdot \boldsymbol{y} + \boldsymbol{E} \cdot \boldsymbol{x} = \boldsymbol{h} \tag{A.6}$$

$$\boldsymbol{x} \geq 0 \tag{A.7}$$

The master problem (P1) is defined by a convex set of feasible solutions and a convex objective function, which allows us to use a Benders decomposition-type algorithm.

Moreover, function $Q(\boldsymbol{y}, \boldsymbol{c_s}, \boldsymbol{F_s})$ has the same structure as the classic slave problem from the Benders decomposition, so the same approximation (and cutting planes selection algorithm) can be used for solving this particular problem as explained in Papavasiliou et al. (2014).

Therefore, the master problem can be re-written, including optimality cuts derived from the Benders algorithm as shown in Eqs. (A.8)–(A.15).

$$(P1') \, Minimize \, z_L \tag{A.8}$$

s.t.:

$$z_L \geq \boldsymbol{d}^{\mathrm{T}} \cdot \boldsymbol{y} \tag{A.9}$$

$$z_L \geq \boldsymbol{d}^{\mathrm{T}} \cdot \boldsymbol{y} + \sum_{s \in S} p_s \cdot \left(\mathrm{Q}\left(\hat{\boldsymbol{y}}^{\boldsymbol{i}}, \boldsymbol{c_s}, \boldsymbol{F_s}\right) + \left(\hat{\boldsymbol{y}}^{\boldsymbol{i}} - \boldsymbol{y}\right)^{\mathrm{T}} \cdot \boldsymbol{F_s}^{\mathrm{T}} \cdot \boldsymbol{u^i_s} \right) \quad 1 \leq i \leq k \tag{A.10}$$

$$v_s \geq \boldsymbol{d}^{\mathrm{T}} \cdot \boldsymbol{y} + \mathrm{Q}\left(\hat{\boldsymbol{y}}^{\boldsymbol{i}}, \boldsymbol{c_s}, \boldsymbol{F_s}\right) + \left(\hat{\boldsymbol{y}}^{\boldsymbol{i}} - \boldsymbol{y}\right)^{\mathrm{T}} \cdot \boldsymbol{F_s}^{\mathrm{T}} \cdot \boldsymbol{u^i_s} - \delta \quad \forall s \in S, 1 \leq i \leq k \tag{A.11}$$

$$\delta + \frac{1}{1-\alpha} \cdot \sum_{s \in S} p_s \cdot v_s \leq \overline{\mathrm{CVaR}} \tag{A.12}$$

$$v_s \geq 0 \quad \forall s \in S \tag{A.13}$$

$$\boldsymbol{y} \in \boldsymbol{Y} \tag{A.14}$$

$$\delta \geq 0 \tag{A.15}$$

Auxiliary variables v_s are used for obtaining the linear form of constraint (A.2) and $\boldsymbol{u^i_s}$ are the Lagrange multipliers of P2$_s$ associated with the coupling constraints (i.e. generation capacities), considering the ith investment decision trial $\hat{\boldsymbol{y}}^{\boldsymbol{i}}$. Constraint (A.9) is added to avoid unboundedness.

Using P1' and P2$_s$ shown in Eqs. (A.5)–(A.15), the following algorithm is proposed:

Step 0: Set $k = 1$. Initialize $\hat{z}_{lower} = -\infty$, $\hat{c}_{lower} = -\infty$ and $\hat{\boldsymbol{y}}^1$. Go to step 1.

Step 1: Solve P1'. Set $\hat{\boldsymbol{y}}^k$ equal to the optimal first-stage solution and set $\hat{z}_{lower} = \hat{z}_L$ and $\hat{c}_{lower} = \hat{\delta} + 1/(1-\alpha) \cdot \sum_{s \in S} p_s \cdot \hat{v}_s$. Go to step 2.

Step 2: For all $s \in S$, solve P2$_s$ using $\hat{\boldsymbol{y}}^k$ as input. Set $\boldsymbol{u}^k_s$ equal to the optimal multipliers of the coupling constraints in Eq. (A.6). Set $\hat{z}_{upper} = \boldsymbol{d}^{\mathrm{T}} \cdot \hat{\boldsymbol{y}}^k + \sum_{s \in S} p_s \cdot \mathrm{Q}(\hat{\boldsymbol{y}}^k, \boldsymbol{c_s}, \boldsymbol{F_s})$ and $\hat{c}_{upper} = CVaR_\alpha(\boldsymbol{C}(\hat{\boldsymbol{y}}^k), \boldsymbol{\rho})$.

Where $CVaR_\alpha(\boldsymbol{x}, \boldsymbol{\rho})$ is the function that computes the $(1-\alpha)$ percentile conditional value at risk of the cost vector $\boldsymbol{x}$ with the associated probabilities vector $\boldsymbol{\rho}$. $\boldsymbol{C}(\hat{\boldsymbol{y}}^k)$ corresponds to the vector containing the total costs of every scenario computed when solving P2$_s$ slaves, given the first-stage decision $\hat{\boldsymbol{y}}^k$ and $\boldsymbol{\rho}$ is the vector containing scenarios' probabilities. Go to step 3.

Step 3: If (i) $|\hat{z}_{upper} - \hat{z}_{lower}| \leq \varepsilon_1$ and (ii) $|\hat{c}_{upper} - \hat{c}_{lower}| \leq \varepsilon_2$ then exit with $\hat{\boldsymbol{y}}^k$ as the optimal solution. Otherwise, set $k = k + 1$ and go to step 1. Note that (ii) can be re-written as $\hat{c}_{upper} - \overline{CVaR} \leq \varepsilon_2$ and $\hat{z}_{upper}$ is not a true upper bound of the real cost expectation until (ii) is fully met.

In the above algorithm, the exit criterion ensures that both cost expectation and CVaR are correctly approximated in the neighborhood of the optimal solution and given that subproblems are linear, convergence is ensured in a finite number of iterations (since true cost expectation and CVaR functions are piecewise linear). For the sake of

simplicity, the addition of Benders feasibility cuts is not explained, al-
though they might be necessary for obtaining the optimal solution.
The addition of these cuts can be done as in the classical Benders decom-
position algorithm. Note also that parallel processing can be used to un-
dertake step 2.

References

Awerbuch, S., 2006. Portfolio-based electricity generation planning: policy implications
    for renewables and energy security. Mitig. Adapt. Strateg. Glob. Chang. 11, 693–710.
Awerbuch, S., Berger, M., 2003. EU Energy Diversity and Security: Applying Portfolio
    Theory to Electricity Planning and Policy-Making. (EET/2003/03).
Bar-Lev, D., Katz, S., 1976. A portfolio approach to fossil fuel procurement in the electric
    utility industry. J. Financ. 31, 933–947.
Bazilian, M., Roques, F., 2008. Analytical Methods for Energy Diversity and Security:
    Portfolio Optimization in the Energy Sector: A Tribute to the Work of Dr. Shimon
    Awerbuch. Elsevier ((October 2008). ISBN-13: 978-0-08-056887-4).
Bessembinder, H., 1992. Systematic risk, hedging pressure, and risk premiums in futures
    markets. Rev. Financ. Stud. 5, 637–667.
Borenstein, S., 2012. The private and public economics of renewable electricity genera-
    tion. J. Econ. Perspect. 26 (1), 67–92.
Chávez, H., Baldick, R., 2012. Inertia and Governor Ramp Rate Constrained Economic
    Dispatch to Assess Primary Frequency Response Adequacy. International Conference
    on Renewable Energies and Power Quality (ICREPQ'12) Santiago de Compostela,
    Spain, March 28–30.
Chávez, H., Baldick, R., Sharma, S., 2014. Governor rate-constrained OPF for primary
    frequency control adequacy. IEEE Trans. Power Syst. 99.
De Jonghe, C., Delarue, E., Belmans, R., D'haeseleer, W., 2010. Determining optimal
    electricity technology mix with high level of wind power penetration. Appl. Energy
    88, 2231–2238.
Delarue, E., De Jonghe, C., Belmans, R., D'haeseleer, W., 2011. Applying portfolio theory to
    the electricity sector: energy versus power. Energy Econ. 33 (1), 12–23.
Denholm, P., Margolis, R., 2007. Evaluating the limits of solar photovoltaics (PV) in
    traditional electric power systems. Energy Policy 35 (5), 2852–2861.
Doherty, R., Outhred, H., O'Malley, M., 2006. Establishing the role that wind generation
    may have in future generation portfolios. IEEE Trans. Power Syst. 21 (3), 1415–1422.
Eide, J., de Sisternes, F., Herzog, H., Webster, M., 2014. CO_2 emission standards and invest-
    ment in carbon capture. Energy Econ. 45, 53–65.
Energy Information Administration, 2015. Assumptions to the Annual Energy Outlook.
    U.S. Department of Energy. Available online at: http://www.eia.gov/forecasts/aeo/
    assumptions/pdf/0554(2015).pdf (Accessed on: March, 2016).
Energy Information Administration, 2014a. Natural gas prices (exports price as LNG). U.S.
    Department of Energy. Available online at: http://www.eia.gov/dnav/ng/ng_pri_
    sum_dcu_nus_a.htm (Accessed on: June, 2014).
Energy Information Administration, 2014b. Petroleum and other liquids. U.S. Department
    of Energy. Available online at: http://www.eia.gov/dnav/pet/pet_pri_spt_s1_m.htm
    (Accessed on: June, 2014).
Energy Information Administration, 2014c. Coal statistics (prices back to 1949). U.S. De-
    partment of Energy. Available online at: http://www.eia.gov/coal/data.cfm#prices
    (Accessed on: June, 2014).
Erb, C., Campbell, H., 2006. The strategic and tactical value of commodity futures. Financ.
    Anal. J. 62, 69–97.
FICO, 2014. Xpress optimization suite. Available online at: http://www.fico.com/en/
    products/fico-xpress-optimization-suite.
Gil, E., Aravena, I., Cárdenas, R., 2014. Generation capacity expansion planning under
    hydro uncertainty using stochastic mixed integer programming and scenario reduc-
    tion. IEEE Trans. Power Syst. (in press).
Gorton, G., Hayashi, F., Geert, K., 2013. The fundamentals of commodity futures returns.
    Rev. Finan. 17 (1), 35–105.
Gotham, D., Muthuraman, K., Preckel, P., Rardin, R., Ruangpattana, S., 2009. A load factor
    based mean–variance analysis for fuel diversification. Energy Econ. 31, 249–256.
Gowrisankaran, G., Reynolds, S.S., Samano, M., 2011. Intermittency and the Value of
    Renewable Energy (no. w17086). National Bureau of Economic Research.
Huang, Y.H., Wu, J.H., 2008. A portfolio risk analysis on electricity supply planning. Energ
    Policy 36, 627–641.
Hull, J., 2009. Options, Futures, and Other Derivatives. seventh ed. Pearson Prentice Hall.
International Energy Agency, 2010. Renewable energy essentials: hydropower. Available
    online at: http://www.iea.org/publications/freepublications/publication/hydropower_
    essentials.pdf (Accessed on: March, 2016).

Jansen, J., Beurskens, L., van Tilburg, X., 2006. Application of Portfolio Analysis to the
    Dutch Generating Mix. (ECN-C--05-100).
Joskow, P., 2011. Comparing the costs of intermittent and dispatchable electricity gener-
    ating technologies. Am. Econ. Rev. Pap. Proc. 100 (3), 238–241.
Kolb, R., 1992. Is normal backwardation normal? J. Futur. Mark. 12 (1), 75–91.
Markowitz, H., 1952. Portfolio selection. J. Financ. 7, 77–91.
Ministry of Energy, 2015. Proceso Participativo de Política Energética 2050 – Mesa ERNC.
    Available online at:. (http://www.energia2050.cl/documentos. Accessed on: March,
    2016).
National Energy Commission, 2014a. Fijación de Precios de Nudo Abril de 2014, Sistema
    Interconectado Central (SIC). Tech. Rep.CNE, Santiago, Chile (Available on-line at:
    http://www.cne.cl/tarificacion/electricidad/precios-de-nudo-de-corto-plazo/abril-
    2014. Accessed on: July, 2014)
National Energy Commission, 2014b. Norma Técnica de Seguridad y Calidad de Servicio.
    CNE, Santiago (Available online at: http://www.cne.cl/images/stories/normativas/
    otros%20niveles/electricidad/Norma%20T%C3%A9cnica%202014/NT%20de%20SyCS_
    2014_Res.%20Exta.%20315.pdf. Accessed on: July, 2014).
National Energy Commission, 2016. Capacidad Instalada de Generación. CNE, Santiago,
    Chile (Available online at: http://www.cne.cl/wp-content/uploads/2015/05/
    capacidad_instalada_de_generaci%C3%B3n.xls. Accessed on: January, 2016).
National Grid, 2014. What are reserve services? United Kingdom. Available online at:
    http://www2.nationalgrid.com/uk/services/balancing-services/reserve-services/
    (Accessed on: September, 2014)
Neuhoff, K., Ehrenmann, A., Butler, L, Cust, J., Hoexter, H., Keats, K., 2008. Space and time:
    wind in an investment planning model. Energy Econ. 30 (4), 1990–2008.
Papadaskalopoulos, D., Strbac, G., Mancarella, P., Aunedi, M., Stanojevic, V., 2013.
    Decentralized participation of flexible demand in electricity markets—part II: applica-
    tion with electric vehicles and heat pump systems. IEEE Trans. Power Syst. 28 (4),
    3667–3674.
Papavasiliou, A., He, Y., Svoboda, A., 2014. Self-commitment of combined cycle units
    under electricity price uncertainty. IEEE Transactions on Power Systems 30 (4),
    1690–1701.
Pérez-Arriaga, I.J., Battle, C., 2012. Impacts of intermittent renewables on electricity gen-
    eration system operation. Econ. Energy Environ. Policy 1 (2), 3–18.
Pindyck, R., 2013. Climate change policy: what do the models tell us? J. Econ. Lit. 51,
    860–872.
Rockafellar, R., Uryasev, S., 2002. Conditional value-at-risk for general loss distributions.
    J. Bank. Financ. 26, 1443–1471.
Roques, F.A., Newbery, D.M., Nuttall, W.J., 2008. Fuel mix diversification incentives in lib-
    eralized electricity markets: a mean–variance portfolio theory approach. Energy
    Econ. 30 (4), 1831–1849.
Silva, V., 2010. Value of Flexibility in Systems with Large Wind Penetration Ph.D. thesis
    Imperial College London (Available online at: http://tel.archives-ouvertes.fr/docs/
    00/72/43/58/PDF/VSilva_PhDAllChapters_v9_-_unlinked_-_test.pdf. Accessed on:
    March, 2014).
Steffen, B., Weber, C., 2013. Efficient storage capacity in power systems with thermal and
    renewable generation. Energy Econ. 36, 556–567.
Strbac, G., 2008. Demand side management: benefits and challenges. Energ Policy 36
    (12), 4419–4426.
Strbac, G., Shakoor, A., Black, M., Pudjianto, D., Bopp, T., 2006. Impact of wind generation
    on the operation and development of the UK electricity systems. Electr. Power Syst.
    Res. 77, 1214–1227.
Sunderkötter, M., Weber, C., 2012. Valuing fuel diversification in power generation capac-
    ity planning. Energy Econ. 34, 1664–1674.
University of Chile, 2014a. Solar Explorer. Available online at: http://ernc.dgf.uchile.cl/
    Explorador/Solar2/ (Accessed on: July, 2014).
University of Chile, 2014b. Wind Explorer. Available online at: http://ernc.dgf.uchile.cl/
    Explorador/Eolico2/ (Accessed on: July, 2014).
Unsihuay-Vila, C., Marangon-Lima, J., Zambroni de Souza, A., Perez-Arriaga, I., Balestrassi,
    P., 2010. A model to long-term, multiarea, multistage, and integrated expansion plan-
    ning of electricity and natural gas systems. IEEE Trans. Power Syst. 25 (2),
    1154–1168.
Vithayasrichareon, P., MacGill, I., 2014. Incorporating short-term operational plant con-
    straints into assessments of future electricity generation portfolios. Appl. Energy
    128, 144–156.
World Energy Council, 2015. World Energy Resources: Charting the Upsurge in Hydropower
    Development. Available online at: https://www.worldenergy.org/publications/2015/
    2015-hydropower-status/ (Accessed on: March, 2016).